Sensitivity analysis for an elemental sulfur-based two-step denitrification model

A. Kostrytsia, S. Papirio, M. R. Mattei, L. Frunzo, P. N. L. Lens and G. Esposito

ABSTRACT

A local sensitivity analysis was performed for a chemically synthesized elemental sulfur (S^0)-based two-step denitrification model, accounting for nitrite (NO_2^-) accumulation, biomass growth and S^0 hydrolysis. The sensitivity analysis was aimed at verifying the model stability, understanding the model structure and individuating the model parameters to be further optimized. The mass specific area of the sulfur particles ($a*$) and hydrolysis kinetic constant (k_1) were identified as the dominant parameters on the model outputs, i.e. nitrate (NO_3^-), NO_2^- and sulfate (SO_4^{2-}) concentrations, confirming that the microbially catalyzed S^0 hydrolysis is the rate-limiting step during S^0-driven denitrification. Additionally, the maximum growth rates of the denitrifying biomass on NO_3^- and NO_2^- were detected as the most sensitive kinetic parameters.

Key words | biological surface-based hydrolysis, elemental sulfur, mathematical modeling, sensitivity analysis, two-step autotrophic denitrification

A. Kostrytsia (corresponding author)
G. Esposito
Department of Civil and Mechanical Engineering,
University of Cassino and Southern Lazio,
via Di Biasio 43, 03043 Cassino, FR,
Italy
E-mail: kostritsia@gmail.com

S. Papirio
Department of Civil, Architectural and
 Environmental Engineering,
University of Naples Federico II,
via Claudio 21, 80125 Naples,
Italy

M. R. Mattei
L. Frunzo
Department of Mathematics and Applications
 Renato Caccioppoli,
University of Naples Federico II,
via Cintia, Monte S. Angelo, 1-80126 Naples,
Italy

P. N. L. Lens
UNESCO-IHE, Institute for Water Education,
P.O. Box 3015, 2601 DA Delft,
The Netherlands

INTRODUCTION

Globally, up to 80% of wastewater is released into the environment without adequate treatment (UN-Water 2015) affecting the water quality in ground and surface water bodies. Contamination by nitrate (NO_3^-) and nitrite (NO_2^-), due to the excessive use of N-based fertilizers and uncontrolled discharge of wastewaters, is one of the main environmental concerns (Kilic *et al.* 2014). Elevated NO_3^- concentrations result in eutrophication and ecological disturbance, while NO_2^- leads to toxicity towards aquatic life. Also, a high NO_3^- concentration imposes an adverse effect on human health such as methemoglobinemia (also known as 'blue baby' syndrome) or higher risk of cancer (Liu *et al.* 2016). Thus, the guidance value of 50 mg/l for NO_3^- was set for drinking water (WHO 2011).

NO_3^- and NO_2^- removal from wastewaters and drinking water can be performed by physico-chemical or biological processes. However, due to high costs and energy demand of the physico-chemical methods (Sierra-Alvarez *et al.*

2007), biological removal of NO_3^- (denitrification) and NO_2^- (denitritation) represents a valuable alternative technology (Mattei *et al.* 2015). Heterotrophic denitrification which uses organic compounds as energy source is a proven technology (Papirio *et al.* 2014; Zou *et al.* 2014), widely applied at the industrial scale. Notwithstanding, autotrophic denitrification has been suggested as an alternative and environmentally sustainable treatment for waters poor in carbon content, due to the costly supplementation of organics (Zhou *et al.* 2015). The use of S^0 as electron donor is easy handling and results in low operational costs and a low N_2O production (Soares 2002; Christianson *et al.* 2015). Therefore, reduced capital and operational costs, a decreased sludge production and limited greenhouse gas emissions (Kilic *et al.* 2014; Di Capua *et al.* 2015) make S^0-based autotrophic denitrification an appropriate technology to be applied in decentralized and small-scale wastewater treatment systems.

However, chemically synthesized S^0 has a low solubility, which limits its application in autotrophic denitrification and denitritation systems. To obtain higher denitrification rates, the use of smaller and more porous S^0 particles, with a higher specific surface area, has previously been suggested (Di Capua *et al.* 2016). The specific surface area of the S^0 particles, thus, becomes one of the key parameters that control the autotrophic denitrification and denitritation rates (Sierra-Alvarez *et al.* 2007).

Modeling has proven to be an important tool for the understanding, design and control of autotrophic denitrification. Over the last years, several mathematical models accounting for S^0-driven autotrophic denitrification have been proposed. In most of them, zero- or half-order reactions have been applied to describe the simplified S^0-driven autotrophic denitrification kinetics without accounting for microbial growth or NO_2^- evolution (Koenig & Liu 2001; Moon *et al.* 2004; Qambrani *et al.* 2015). Xu *et al.* (2016) established a kinetic model for two-step autotrophic denitrification with hydrogen sulfide (H_2S) that accurately predicted the concentration of the intermediate NO_2^-. Recently, Liu *et al.* (2016) have developed a model for three-step autotrophic denitrification linked to H_2S and S^0 oxidation with a focus on N_2O accumulation.

However, none of the above mentioned models distinctly focused on S^0 hydrolysis as a step prior to autotrophic denitrification and denitritation (Sierra-Alvarez *et al.* 2007). In a recent study, a mechanistic model accounting for NO_2^- accumulation, biomass growth and S^0 hydrolysis has been proposed (Kostrytsia *et al.* 2018). As demonstrated through numerical simulations, the developed model could serve as a tool to predict the performance of autotrophic denitrification biofilm systems and assess their process efficiency when compared to other denitrification systems. In the present work, the model developed by Kostrytsia *et al.* (2018) was subjected to a sensitivity analysis to verify the model stability as well as identify the model parameters to be further optimized. Specifically, the focus was to use a local sensitivity analysis to better understand the dominant parameters of the process.

METHODS

Mathematical model overview

A mathematical model was developed by Kostrytsia *et al.* (2018) to dynamically simulate the main processes occurring during the two-step denitrification with S^0 (S_1). The model takes into account the activities of a hydrolytic biomass (X_1) growing on S^0 lentils and an autotrophic denitrifying biomass (X_2) using NO_3^- (S_3) or NO_2^- (S_4) as electron acceptor and reducing them to dinitrogen gas (N_2) (S_5), and evaluates the interactions between S^0 hydrolysis and S^0-based denitrification and denitritation. S^0 uptake was modeled by introducing a new variable, the bioavailable sulfur (S_2), which is the soluble compound directly taken up by the denitrifying bacteria for further oxidation to SO_4^{2-} (S_6). A modified surface-based kinetic equation was introduced to account for the hydrolysis of S^0 (Esposito *et al.* 2008). The model equations were derived from mass balances and expressed as double-Monod kinetics (Equations (1)–(8)), as reported below or in the matrix in Table 1.

$$\frac{dS_1}{dt} = -k_1 \frac{S_1}{\frac{K_1}{a^*} + S_1} X_1, \tag{1}$$

$$\frac{dS_2}{dt} = k_1 \frac{S_1}{\frac{K_1}{a^*} + S_1} X_1 - \frac{r_1}{Y_{2,3}} \mu_{2,3}^{max} \frac{S_2}{K_{2,2} + S_2}$$
$$\frac{(S_3 - S_3^*)}{K_{2,3} + (S_3 - S_3^*)} \frac{S_3}{S_3 + S_4} X_2 - \frac{r_2}{Y_{2,4}} \mu_{2,4}^{max}$$
$$\frac{S_2}{K_{2,2} + S_2} \frac{(S_4 - S_4^*)}{K_{2,4} + (S_4 - S_4^*)} \frac{S_4}{S_3 + S_4} X_2, \tag{2}$$

$$\frac{dS_3}{dt} = -\frac{1}{Y_{2,3}} \mu_{2,3}^{max} \frac{S_2}{K_{2,2} + S_2} \frac{(S_3 - S_3^*)}{K_{2,3} + (S_3 - S_3^*)} \frac{S_3}{S_3 + S_4} X_2, \tag{3}$$

$$\frac{dS_4}{dt} = \frac{1}{Y_{2,3}} \mu_{2,3}^{max} \frac{S_2}{K_{2,2} + S_2} \frac{(S_3 - S_3^*)}{K_{2,3} + (S_3 - S_3^*)} \frac{S_3}{S_3 + S_4} X_2$$
$$-\frac{1}{Y_{2,4}} \mu_{2,4}^{max} \frac{S_2}{K_{2,2} + S_2} \frac{(S_4 - S_4^*)}{K_{2,4} + (S_4 - S_4^*)} \frac{S_4}{S_3 + S_4} X_2, \tag{4}$$

$$\frac{dS_5}{dt} = \frac{1}{Y_{2,4}} \mu_{2,4}^{max} \frac{S_2}{K_{2,2} + S_2} \frac{(S_4 - S_4^*)}{K_{2,4} + (S_4 - S_4^*)} \frac{S_4}{S_3 + S_4} X_2, \tag{5}$$

$$\frac{dS_6}{dt} = \frac{r_1}{Y_{2,3}} \mu_{2,3}^{max} \frac{S_2}{K_{2,2} + S_2} \frac{(S_3 - S_3^*)}{K_{2,3} + (S_3 - S_3^*)} \frac{S_3}{S_3 + S_4} X_2$$
$$+ \frac{r_2}{Y_{2,4}} \mu_{2,4}^{max} \frac{S_2}{K_{2,2} + S_2} \frac{(S_4 - S_4^*)}{K_{2,4} + (S_4 - S_4^*)} \frac{S_4}{S_3 + S_4} X_2, \tag{6}$$

$$\frac{dX_1}{dt} = K_0 k_1 \frac{S_1}{\frac{K_1}{a^*} + S_1} X_1 - k_{d,1} X_1, \tag{7}$$

$$\frac{dX_2}{dt} = \mu_{2,3}^{max} \frac{S_2}{K_{2,2} + S_2} \frac{(S_3 - S_3^*)}{K_{2,3} + (S_3 - S_3^*)} \frac{S_3}{S_3 + S_4} X_2$$
$$+ \mu_{2,4}^{max} \frac{S_2}{K_{2,2} + S_2} \frac{(S_4 - S_4^*)}{K_{2,4} + (S_4 - S_4^*)} \frac{S_4}{S_3 + S_4} X_2 - k_{d,2} \cdot X_2 \tag{8}$$

where K_0 denotes the efficiency growth coefficient for hydrolytic biomass; r_1 and r_2 are the stoichiometric S_2 to

Table 1 | Stoichiometric matrix used for the mathematical modeling of two-step autotrophic denitrification with S^0 (adopted from Kostrytsia et al. (2018))

A_{ij} i component → j process ↓	S_1[a] (mg S/l)	S_2[b] (mg S/l)	S_3[c] (mg N/l)	S_4[d] (mg N/l)	S_5[e] (mg N/l)	S_6[f] (mg N/l)	X_1[g] (mg VS/l)	X_2[h] (mg VS/l)	Rate (mg VS/l·d)
1. Hydrolysis of S_1	-1	1					K_0		$k_1 \dfrac{S_1}{\dfrac{K_1}{a^*}+S_1}X_1$
2. Autotrophic growth on S_3		$-\dfrac{r_1}{Y_{2,3}}$	$-\dfrac{1}{Y_{2,3}}$	$\dfrac{1}{Y_{2,3}}$		$\dfrac{r_1}{Y_{2,3}}$		1	$\mu_{2,3}^{max}\dfrac{S_2}{K_{2,2}+S_2}\dfrac{(S_3-S_3^*)}{K_{2,3}+(S_3-S_3^*)}\dfrac{S_3}{S_3+S_4}X_2$
3. Autotrophic growth on S_4		$-\dfrac{r_2}{Y_{2,4}}$		$-\dfrac{1}{Y_{2,4}}$	$\dfrac{1}{Y_{2,4}}$	$\dfrac{r_2}{Y_{2,4}}$		1	$\mu_{2,4}^{max}\dfrac{S_2}{K_{2,2}+S_2}\dfrac{(S_4-S_4^*)}{K_{2,4}+(S_4-S_4^*)}\dfrac{S_4}{S_3+S_4}X_2$
4. Decay of X_1							-1		$k_{d,1}X_1$
5. Decay of X_2								-1	$k_{d,2}X_2$

[a]Elemental sulfur.
[b]Bioavailable sulfur.
[c]Nitrate.
[d]Nitrite.
[e]Nitrogen gas.
[f]Sulfate.
[g]Hydrolytic biomass.
[h]Denitrifying biomass.
VS: volatile solids.

S_3 and S_2 to S_4 ratios, respectively; $Y_{2,3}$ and $Y_{2,4}$ represent the denitrifying biomass yield coefficients on NO_3^- and NO_2^-, respectively; a^* denotes the mass specific area of the sulfur particles; k_1 denotes the hydrolysis kinetic constant; K_1 indicates the volume specific half-saturation constant for S^0; $\mu_{2,3}^{max}$ and $\mu_{2,4}^{max}$ represent the maximum growth rates for denitrifying biomass on NO_3^- and NO_2^-, respectively; $k_{d,1}$ and $k_{d,2}$ represent the decay constants for X_1 and X_2 biomass, respectively; $K_{2,2}$, $K_{2,3}$ and $K_{2,4}$ denote the half-saturation constants for S^0, NO_3^- and NO_2^-, respectively; S_3^* and S_4^* indicate the lowest NO_2^- and NO_3^- concentrations that enable metabolic activities of X_2. The obtained ordinary differential equations (ODEs) were integrated by using an original software developed on the MATLAB platform and based on the numerical differentiation formulas.

The general structure of the described model is illustrated in Figure 1. Two main compartments can be individuated: the first one is related to the two-step denitrification kinetic reaction system, the second one represents the microbially catalyzed hydrolysis reaction system. The model parameters have been classified in three main groups: kinetic ($\mu_{2,3}^{max}$, $\mu_{2,4}^{max}$, $k_{d,2}$, $K_{2,2}$, $K_{2,3}$, $K_{2,4}$, S_3^* and S_4^*) and stoichiometric ($Y_{2,3}$, $Y_{2,4}$, r_1 and r_2), which directly affect the two-step denitrification kinetic reaction system ('biological kinetic reaction system' in Figure 1), and hydrolysis parameters (K_0, a^*, k_1, K_1 and $k_{d,1}$) which are related to the S^0 hydrolysis compartment. K_0 represents the efficiency

growth coefficient for X_1; r_1 and r_2 are the stoichiometric S_2 to S_3 and S_2 to S_4 ratios, respectively. The values of $Y_{2,3}$, $Y_{2,4}$, $K_{2,2}$, $K_{2,4}$, r_1, r_2, $k_{d,1}$ and $k_{d,2}$ were adopted from previous studies (Sierra-Alvarez et al. 2007; Sin et al. 2008; Liu et al. 2016; Xu et al. 2016) (Table 2). The optimal values of $\mu_{2,3}^{max}$ and $\mu_{2,4}^{max}$ were deducted from both the denitrification and denitritation experiments (Table 2).

Sensitivity analysis

The model proposed by Kostrytsia et al. (2018) requires a high dimensional (stoichiometric, kinetic and hydrolysis-related) parameter space to be explored. To estimate each parameter, excess experimental results should be provided to avoid ill-conditioning of the parameter estimation (Kesavan & Law 2005). Therefore, a model sensitivity analysis was performed to identify the parameter targets for further experimental exploration (Jarrett et al. 2015). The low-sensitive parameters have a negligible effect on the predictions, whereas the highly sensitive parameters require some level of certainty to make robust model predictions (Croicu et al. 2017).

In this model, a local sensitivity analysis was performed to compute sensitivity functions for the dynamic simulations with the initial conditions of 30 mg/l NO_2^--N and 210 mg/l NO_3^--N, originating from the kinetic experiments (Kostrytsia et al. 2018). The stoichiometric ratios (r_1 and r_2) were
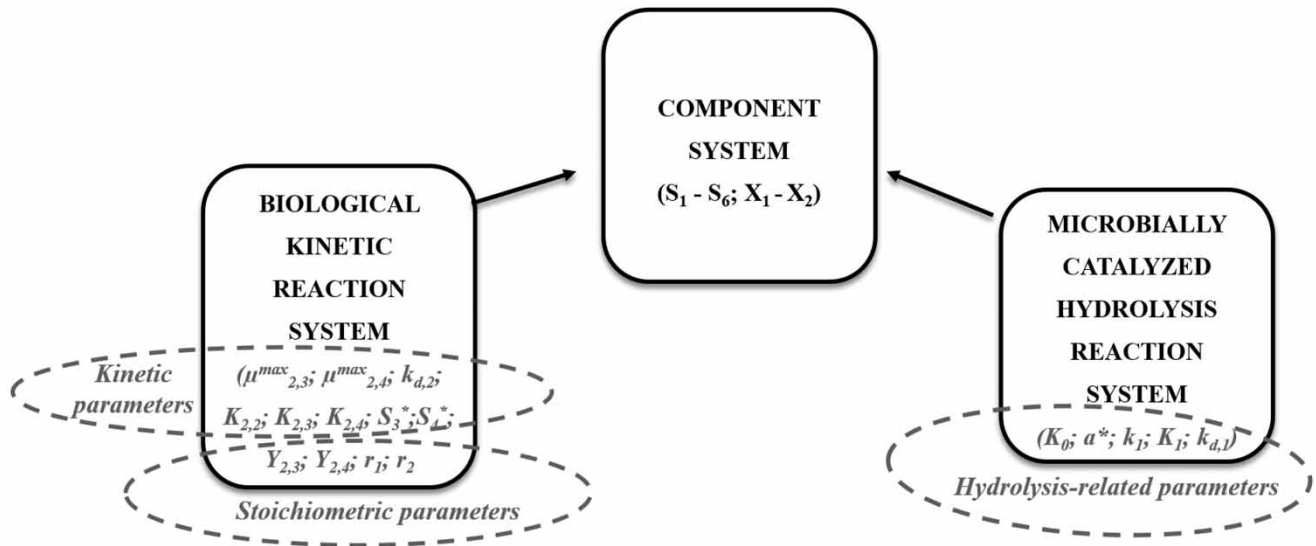
Figure 1 │ General model structure describing the microbially catalyzed S^0 hydrolysis and two-step autotrophic denitrification kinetics. The model parameters influencing each reaction system are mentioned in italics.

Table 2 │ Stoichiometric and kinetic parameters (with nominal values) of the developed model for two-step autotrophic denitrification with S^0 (adopted from Kostrytsia et al. (2018))

Parameter		Value	Unit	Source
Stoichiometric parameters				
$Y_{2,3}$	Yield coefficient for X_2 on S_3	0.25	mg VS/mg N	Xu et al. (2016)
$Y_{2,4}$	Yield coefficient for X_2 on S_4	0.28	mg VS/mg N	Xu et al. (2016)
r_1	S_2 to S_3 stoichiometric ratio	1.2	mg S/mg N	Sierra-Alvarez et al. (2007)
r_2	S_2 to S_4 stoichiometric ratio	0.55	mg S/mg N	Sierra-Alvarez et al. (2007)
Kinetic parameters				
K_0	Efficiency growth coefficient for X_1	0.1	mg VS/mg S	Kostrytsia et al. (2018)
$\mu_{2,3}^{max}$	Maximum growth rate for X_2 on S_3	0.0067	1/d	Kostrytsia et al. (2018)
$\mu_{2,4}^{max}$	Maximum growth rate for X_2 on S_4	0.0058	1/d	Kostrytsia et al. (2018)
$K_{2,2}$	Half-saturation constant for S_2	0.215	mg S/l	Liu et al. (2016)
$K_{2,3}$	Half-saturation constant for S_3	36	mg N/l	Kostrytsia et al. (2018)
S_3^*	The threshold value for S_3	35	mg N/l	Kostrytsia et al. (2018)
$K_{2,4}$	Half-saturation constant for S_4	40	mg N/l	Xu et al. (2016)
S_4^*	The threshold value for S_4	37	mg N/l	Kostrytsia et al. (2018)
K_1	Volume specific half-saturation constant for S_1	5.1	1/dm	Kostrytsia et al. (2018)
k_1	Hydrolysis kinetic constant	0.12	mg S/mg VS d	Kostrytsia et al. (2018)
a^*	Mass specific area	0.0008164	dm^2/mg	Kostrytsia et al. (2018)
$k_{d,1}$	Decay rate coefficient for X_1	0.0006	1/d	Sin et al. (2008)
$k_{d,2}$	Decay rate coefficient for X_2	0.0006	1/d	Sin et al. (2008)

VS: volatile solids.

calculated on the biotransformation mechanism and obtained by previous experimental studies (Sierra-Alvarez et al. 2007). Thus, r_1 and r_2 were not re-estimated in the current study. Additionally, the influence of the biomass decay rates ($k_{d,1}$ and $k_{d,2}$) of the microorganisms performing S^0-driven denitrification and denitritation was out of investigation, as $k_{d,1}$ and $k_{d,2}$ were very low (Liu et al. 2016). Also, the threshold values for NO_3^- and NO_2^- (S_3^* and S_4^*,

respectively), which represent the concentration values below which the microorganisms are not able to grow, were not considered for the sensitivity analysis. Therefore, the sensitivity analysis was conducted for the following 11 parameters: $\mu_{2,3}^{max}$, $\mu_{2,4}^{max}$, $K_{2,2}$, $K_{2,3}$ and $K_{2,4}$ (kinetic), $Y_{2,3}$ and $Y_{2,4}$ (stoichiometric) and K_0, a^*, k_1 and K_1 (hydrolysis-related). NO_3^--N, NO_2^--N and $SO_4^{2-}-S$ concentrations were set as the focused variables to measure the sensitivity.

The sensitivities were calculated as the effect of the change in the input parameters on the model output over a time span of 22 days. An automatic differentiation tool SENS_SYS coupled with the ODE solver of MATLAB was used to predict the local sensitivity. The SENS_SYS tool is an extension of the ODE15s tool that allows the solving of the ODE system while computing derivatives (sensitivities) of the solution with respect to parameters (Molla & Padilla 2002). The accuracy of the SENS_SYS tool is controlled by the default relative tolerance of 1×10^{-6}. The sensitivity analysis of the system F was calculated by differentiating the system with respect to the kinetic parmeter u, as illustrated in Equation (9).

$$F(t, y, y', u) = 0 \qquad (9)$$

where t denotes the time interval for the integration (days), y represents the input state variable, y' the first derivative of y with respect to t, and u denotes the parameter.

RESULTS AND DISCUSSION

Parameter sensitivity overview on NO_3^--N, NO_2^--N and $SO_4^{2-}-S$ concentrations

The absolute sensitivities of the 11 parameters (K_0, $Y_{2,3}$, $Y_{2,4}$, a^*, k_1, K_1, $\mu_{2,3}^{max}$, $\mu_{2,4}^{max}$, $K_{2,2}$, $K_{2,3}$ and $K_{2,4}$) to the input state variables (i.e. 210, 0 and 0 mg/L of NO_3^--N, NO_2^--N and $SO_4^{2-}-S$, respectively) are shown in Figure 2. The nominal values of the parameters used for the model (Equations (1)–(8)) are listed in Table 2.

The $Y_{2,3}$, $Y_{2,4}$, a^*, k_1, $\mu_{2,3}^{max}$, $\mu_{2,4}^{max}$ and $K_{2,2}$ parameters were sensitive to some extent to at least one of the model outputs, i.e. NO_3^--N, NO_2^--N and $SO_4^{2-}-S$ (Figure 2). Both NO_3^--N and NO_2^--N process variables were highly sensitive to a^*, $\mu_{2,3}^{max}$ and $\mu_{2,4}^{max}$. It is noteworthy to highlight that a negative value of the absolute sensitivity refers to the reduction of the process variables with parameter perturbation. For example, the
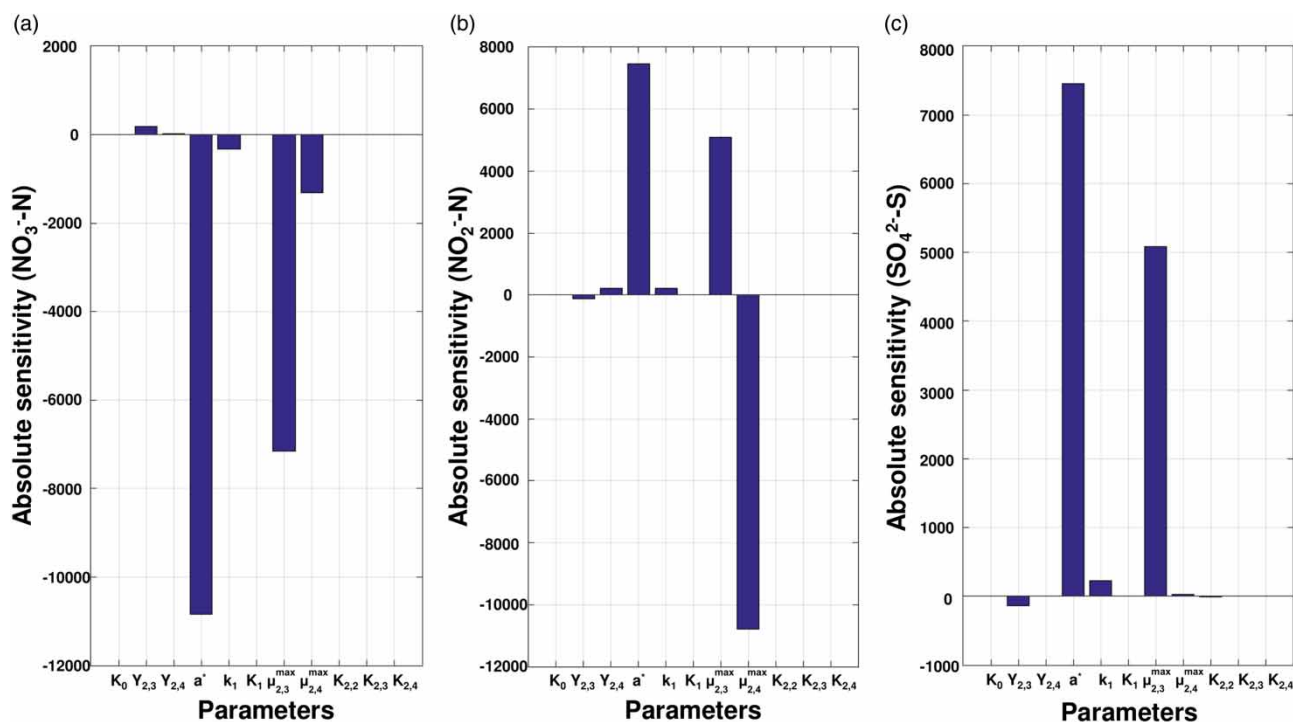

Figure 2 │ Absolute (or local) sensitivities of kinetic parameters during the simulation time for the degradation of (a) NO_3^--N and (b) NO_2^--N and the production of (c) $SO_4^{2-}-S$.

negative value of $\mu_{2,3}^{max}$ sensitivity for NO_3^--N indicated NO_3^--N consumption (Figure 2(a)), while the positive value of $\mu_{2,3}^{max}$ sensitivity for NO_2^--N corresponded to NO_2^--N production (Figure 3(a)). The NO_3^- and NO_2^- reduction was coupled to S^0 biooxidation in order to produce energy and facilitate microbial growth. Therefore, the use of NO_3^- or NO_2^- as a substrate for the microbial cultures resulted in a high sensitivity of the $\mu_{2,3}^{max}$ and $\mu_{2,3}^{max}$ to the model outputs (Figure 2).

The sensitivity analysis results suggest that the parameter vector can be reduced to a^*, k_1, $\mu_{2,3}^{max}$ and $\mu_{2,4}^{max}$, based on the minimum magnitude of significance considered (200 as absolute sensitivity). The parameters deemed not to be sufficiently significant can be fixed at their nominal values (Table 2). Further investigation might be related to such a reduced model both in terms of assumed parameter distribution and experimental calibration. Further calibration is required for the most sensitive model parameters to improve the quality of the model. However, the values of absolute sensitivity for K_0, K_1, $K_{2,3}$ and $K_{2,4}$ for each process variable were significantly lower than those of $Y_{2,3}$, $Y_{2,4}$, a^*, k_1, $\mu_{2,3}^{max}$, $\mu_{2,4}^{max}$ and $K_{2,2}$. The effect of each sensitive parameter on the process variables should be investigated in more detail due to their crucial role in the model calibration.

Sensitivity analysis for kinetic ($\mu_{2,3}^{max}$, $\mu_{2,4}^{max}$, $K_{2,2}$, $K_{2,3}$ and $K_{2,4}$) and stoichiometric ($Y_{2,3}$ and $Y_{2,4}$) model parameters

To investigate the effect of each parameter on the process variables, a series of sensitivity curves was obtained by changing the five kinetic ($\mu_{2,3}^{max}$, $\mu_{2,4}^{max}$, $K_{2,2}$, $K_{2,3}$ and $K_{2,4}$), and the two stoichiometric ($Y_{2,3}$ and $Y_{2,4}$) parameters one by one during the simulation. The effect of each parameter on the input state variables NO_3^--N, NO_2^--N and SO_4^{2-}-S is illustrated in Figure 3. The greater parameter line slope indicates the more significant role of the parameter in the autotrophic denitrification process.

The most sensitive kinetic parameters were the maximum growth rate of the denitrifying biomass on NO_3^- ($\mu_{2,3}^{max}$) and NO_2^- ($\mu_{2,4}^{max}$) as illustrated in Figures 2(a)–2(c) and 3(d)–3(e), with a more significant effect on NO_3^--N from day 10 to day 15 when the denitrification rate was higher (Kostrytsia *et al.* 2018). The SO_4^{2-}-S absolute sensitivity was 10,000 and 7,500 for $\mu_{2,3}^{max}$ and $\mu_{2,4}^{max}$ (Figure 2), respectively. This was likely attributed to the higher metabolic rates, in particular S^0 oxidation to SO_4^{2-}, of the denitrifying bacteria growing on NO_3^- ($\mu_{2,3}^{max}$) rather than on NO_2^-. On the other hand, the half-saturation constants for S_2 ($K_{2,2}$), S_3 ($K_{2,3}$) and S_4 ($K_{2,4}$) had a minimal impact on the model outputs (Figure 3(c), 3(f) and 3(g)). A larger set of experimental data would be required to get an accurate evaluation of the half-saturation constants. More data could be obtained from kinetic tests with different initial substrate concentrations for a reliable model calibration of the half-saturation constants.

Regarding the stoichiometric parameters, the denitrifying biomass yield coefficient on NO_3^- ($Y_{2,3}$) showed a high sensitivity for NO_3^--N, NO_2^--N and SO_4^{2-}-S outputs (Figure 3(a)). The highest sensitivity of the $Y_{2,3}$ was observed between days 10 and 15 due to the higher denitrification rate.
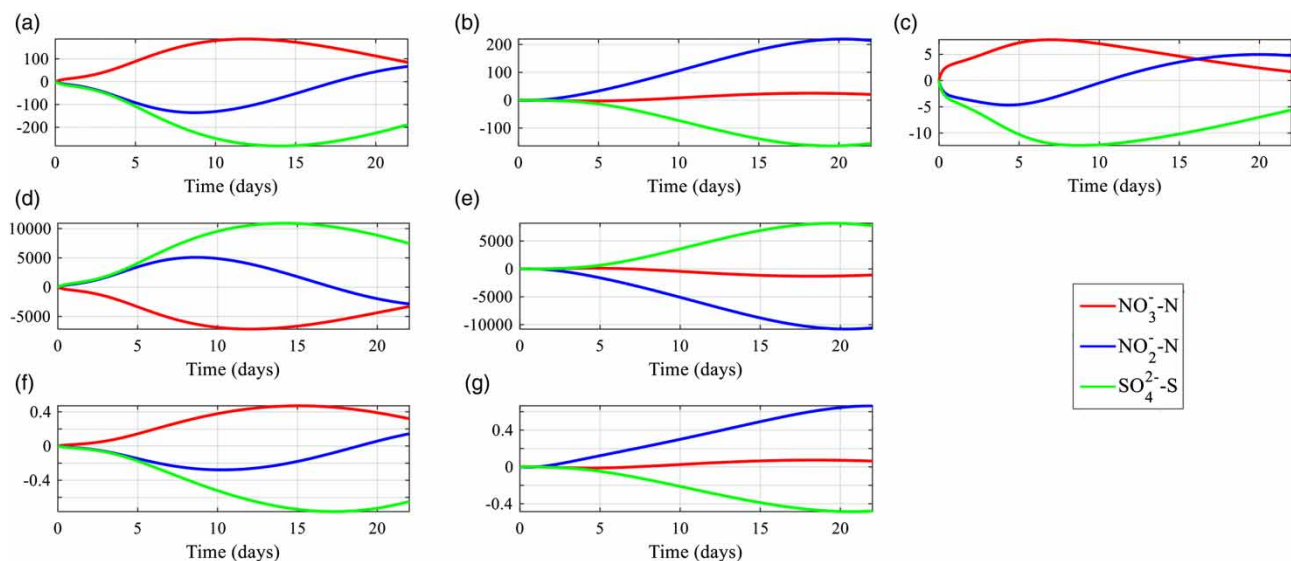

Figure 3 | Output absolute (or local) sensitivity of kinetic and stoichiometric parameters: (a) $Y_{2,3}$, (b) $Y_{2,4}$, (c) $K_{2,2}$, (d) $\mu_{2,3}^{max}$, (e) $\mu_{2,4}^{max}$, (f) $K_{2,3}$ and (g) $K_{2,4}$.
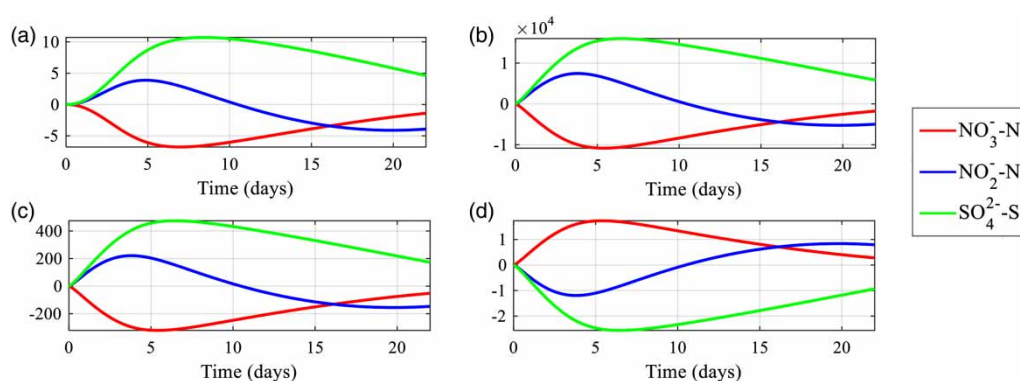
Figure 4 | Output absolute (or local) sensitivity of hydrolysis-related parameters: (a) K_0, (b) a^*, (c) k_1 and (d) K_1.

The effect of $Y_{2,4}$ sensitivity on the NO_2^--N and SO_4^{2-}-S outputs increased with time due to the accumulation of NO_2^--N as an intermediate product of the NO_3^--N degradation.

Sensitivity analysis for hydrolysis-related (K_0, a^*, k_1 and K_1) model parameters

The effect of hydrolysis-related model parameters (K_0, a^*, k_1 and K_1) on the input state variables NO_3^--N, NO_2^--N and SO_4^{2-}-S is illustrated in Figure 4. The mass specific area of the sulfur particles (a^*) posed, apparently, a major influence on the model outputs and was ranked as a first dominant parameter (Figure 2). The parameter a^* accounts for the overall surface area of the sulfur particles to be microbially solubilized prior to denitrification and denitritation. As illustrated in Figure 4(b), the NO_3^--N output was more sensitive to the change in parameter a^*, compared to NO_2^--N. The latter might be attributed to the higher stoichiometric S/N ratio required for complete denitrification than for denitritation. This is consistent with the literature, where the impact of the specific surface area of sulfur particles was suggested as a prerequisite of S^0 oxidation coupled to denitrification (Wang et al. 2016). The model proposed by Kostrytsia et al. (2018) describes the surface-based S^0 hydrolysis as an inevitable aspect and rate-limiting step in the denitrification and denitritation processes, and the high sensitivity of parameter a^* to the model outputs confirmed the significance of the used hydrolysis approach.

Among the other parameters related to the S^0 hydrolysis step, the hydrolysis kinetic constant (k_1), being dependent on the nature of sulfur, possessed a high sensitivity for the model output variables (Figure 4(c)). The absolute sensitivity of both parameters a^* and k_1 showed a peak between days 5 and 10 due to the high denitrification rate, and then slowly dropped (Figure 4(b) and 4(c), respectively). Consequently,

the model predictions and calibration are crucial during that phase. On the other hand, the efficiency growth coefficient for hydrolytic biomass (K_0) and volume specific half-saturation constant for S^0 (K_1) did not significantly influence the model outputs (Figure 4(a) and 4(d), respectively).

CONCLUSIONS

In this work, the results of a local sensitivity analysis performed on a newly developed model for microbially-catalyzed elemental S^0 hydrolysis and two-step denitrification were presented. The sensitivity analysis provided a few insights on the importance of parameter values and their impact on process dynamics. The sensitivity analysis demonstrated that the model was more sensitive to the mass specific area of the sulfur particles (a^*), hydrolysis kinetic constant (k_1) and the maximum growth rate of the denitrifying biomass on NO_3^- ($\mu_{2,3}^{max}$) and NO_2^- ($\mu_{2,4}^{max}$). The high sensitivity of hydrolysis-related parameters (a^* and k_1) to the input state variables (NO_3^--N, NO_2^--N and SO_4^{2-}-S) confirmed the importance of including the microbially catalyzed surface-based S^0 hydrolysis as a limiting process step in the two-step denitrification model. Further experimental and modeling investigations should thus focus on the S^0 hydrolysis.

NOTES

The authors have no competing interests to declare.

REFERENCES

Christianson, L., Lepine, C., Tsukuda, S., Saito, K. & Summerfelt, S. 2015 Nitrate removal effectiveness of fluidized sulfur-based autotrophic denitrification biofilters for recirculating aquaculture systems. *Aquacultural Engineering* **68**, 10–18. doi:10.1016/j.aquaeng.2015.07.002.

Croicu, A. M., Jarrett, A. M., Cogan, N. G. & Hussaini, M. Y. 2017 Short-term antiretroviral treatment recommendations based on sensitivity analysis of a mathematical model for HIV infection of CD^{4+} T cells. *Bulletin of Mathematical Biology* **79** (11), 2649–2671. doi:10.1007/s11538-017-0345-7.

Di Capua, F., Papirio, S., Lens, P. N. L. & Esposito, G. 2015 Chemolithotrophic denitrification in biofilm reactors. *Chemical Engineering Journal* **280**, 643–657. doi:10.1016/j.cej.2015.05.131.

Di Capua, F., Ahoranta, S. H., Papirio, S., Lens, P. N. L. & Esposito, G. 2016 Impacts of sulfur source and temperature on sulfur-driven denitrification by pure and mixed cultures of *Thiobacillus*. *Process Biochemistry* **51**, 1576–1584. doi:10.1016/j.procbio.2016.06.010.

Esposito, G., Frunzo, L., Panico, A. & d'Antonio, G. 2008 Mathematical modelling of disintegration-limited co-digestion of OFMSW and sewage sludge. *Water Science and Technology* **58** (7), 1513–1519. doi:10.2166/wst.2008.509.

Jarrett, A. M., Liu, Y., Cogan, N. G. & Hussaini, M. Y. 2015 Global sensitivity analysis used to interpret biological experimental results. *Journal of Mathematical Biology* **71**, 151–170. doi:10.1007/s00285-014-0818-3.

Kesavan, P. & Law, V. J. 2005 Practical identifiability of parameters in monod kinetics and statistical analysis of residuals. *Biochemical Engineering Journal* **24**, 95–104. doi:10.1016/j.bej.2005.01.028.

Kilic, A., Sahinkaya, E. & Cinar, O. 2014 Kinetics of autotrophic denitrification process and the impact of sulphur/limestone ratio on the process performance. *Environmental Technology* **35**, 2796–2804. doi:10.1080/09593330.2014.922127.

Koenig, A. & Liu, L. H. 2001 Kinetic model of autotrophic denitrification in sulphur packed-bed reactors. *Water Research* **35**, 1969–1978. doi:10.1016/S0043-1354(00)00483-8.

Kostrytsia, A., Papirio, S., Frunzo, L., Mattei, M. R., Porca, E., Collins, G., Lens, P. N. L. & Esposito, G. 2018 Elemental sulfur-based autotrophic denitrification and denitritation: microbially catalyzed sulfur hydrolysis and nitrogen conversions. *Journal of Environmental Management* **211**, 313–322. doi:10.1016/j.jenvman.2018.01.064.

Liu, Y., Peng, L., Ngo, H. H., Guo, W., Wang, D., Pan, Y., Sun, J. & Ni, B. J. 2016 Evaluation of nitrous oxide emission from sulfide- and sulfur-based autotrophic denitrification processes. *Environmental Science and Technology* **50**, 9407–9415. doi:10.1021/acs.est.6b02202.

Mattei, M. R., Frunzo, L., D'Acunto, B., Esposito, G. & Pirozzi, F. 2015 Modelling microbial population dynamics in multispecies biofilms including Anammox bacteria. *Ecological Modelling* **304**, 44–58. doi:10.1016/j.ecolmodel.2015.02.007.

Molla, V. M. G. & Padilla, R. G. 2002 *Description of MATLAB Functions SENS_SYS and SENS_IND*. Universidad Politecnica de Valencia, Spain.

Moon, H. S., Ahn, K. H., Lee, S., Nam, K. & Kim, J. Y. 2004 Use of autotrophic sulfur-oxidizers to remove nitrate from bank filtrate in a permeable reactive barrier system. *Environmental Pollution* **129**, 499–507. doi:10.1016/j.envpol.2003.11.004.

Papirio, S., Ylinen, A., Zou, G., Peltola, M., Esposito, G. & Puhakka, J. A. 2014 Fluidized-bed denitrification for mine waters. Part I: low pH and temperature operation. *Biodegradation* **25**, 417–423. doi:10.1007/s10532-013-9671-0.

Qambrani, N. A., Jung, Y. S., Yang, J. E., Ok, Y. S. & Oh, S.-E. 2015 Application of half-order kinetics to sulfur-utilizing autotrophic denitrification for groundwater remediation. *Environmental Earth Sciences* **73**, 3445–3450. doi:10.1007/s12665-014-3641-7.

Sierra-Alvarez, R., Beristain-Cardoso, R., Salazar, M., Gómez, J., Razo-Flores, E. & Field, J. A. 2007 Chemolithotrophic denitrification with elemental sulfur for groundwater treatment. *Water Research* **41**, 1253–1262. doi:10.1016/j.watres.2006.12.039.

Sin, G., Kaelin, D., Kampschreur, M. J., Takács, I., Wett, B., Gernaey, K. V., Rieger, L., Siegrist, H. & Van Loosdrecht, M. C. M. 2008 Modelling nitrite in wastewater treatment systems: a discussion of different modelling concepts. *Water Science and Technology* **58**, 1155–1171. doi:10.2166/wst.2008.485.

Soares, M. I. M. 2002 Denitrification of groundwater with elemental sulfur. *Water Research* **36**, 1392–1395. doi:10.1016/S0043-1354(01)00326-8.

UN-Water 2015 *Wastewater Management: A UN-Water Analytical Brief*. UN-Water, Geneva, Switzerland.

Wang, Y., Bott, C. & Nerenberg, R. 2016 Sulfur-based denitrification: effect of biofilm development on denitrification fluxes. *Water Research* **100**, 184–193. doi:10.1016/j.watres.2016.05.020.

WHO 2011 *Nitrate and Nitrite in Drinking Water: Background Document for Development of WHO Guidelines for Drinking Water Quality*. WHO, Geneva, Switzerland.

Xu, G., Yin, F., Chen, P. S., Xu, Y. & Yu, P. H. 2016 Mathematical modeling of autotrophic denitrification (AD) process with sulphide as electron donor. *Water Research* **91**, 225–234. doi:10.1016/j.watres.2016.01.011.

Zhou, W., Liu, X., Dong, X., Wang, Z., Yuan, Y., Wang, H. & He, S. 2015 Sulfur-based autotrophic denitrification from the micro-polluted water. *Journal of Environmental Sciences (China)* **44**, 180–188. doi:10.1016/j.jes.2016.01.002.

Zou, G., Papirio, S., Ylinen, A., Di Capua, F., Lakaniemi, A. M. & Puhakka, J. A. 2014 Fluidized-bed denitrification for mine waters. Part II: effects of Ni and Co. *Biodegradation* **25**, 417–423. doi:10.1007/s10532-013-9670-1.